

## Development Status of High Performance Pore Optics

More detailed aspects of some of the development activities are provided in the comprehensive suite of papers presented at the 2006 SPIE Annual Symposium. Links to those papers are provided at:

[http://www.rssd.esa.int/index.php?project=XEUS&page=SPIE\\_Documents](http://www.rssd.esa.int/index.php?project=XEUS&page=SPIE_Documents)

This note provides a brief overview of critical issues and some recent updates since the publication of the above papers.

### 1. Introduction

The science requirements for an X-ray Observatory to be deployed in the post-XMM-Newton and Chandra era have been widely debated. Future spectroscopic investigations will require an enormous increase in collecting area to enable the use of the next generation of advanced spectrometers that will provide the necessary plasma diagnostics capability. A commensurate increase in sensitivity that is necessary to push back the detection of sources to the earliest eras of the Universe, must be accompanied with an angular resolution that prevents confusion of faint sources and allows mapping of source with high dynamic range of brightness.

The Advanced Concepts and Science Payloads Office (SCI-A) of ESA initially worked to extend the existing XMM-Newton mirror technology to reach these goals, but immediately ran into a fundamental limit suffered by all competing telescope technologies. Figure 1 graphically shows for all existing technologies, the trend line for mirror collecting area per unit mass against achievable resolution. The next generation observatory requires an area of several square metres but a realistic launch mass capability limits the mirror payload to 1-2 tonnes. At the same time, the angular resolution requirements (arcseconds) places the performance firmly into the realm only achieved to date with massive figured glass optics.

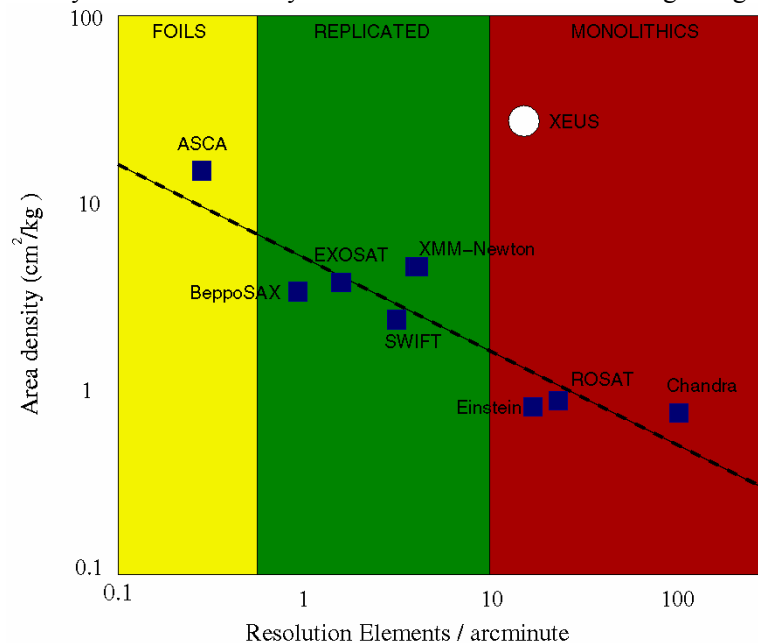


Figure 1. Comparison of resolving power with mass/unit area of existing telescope designs shows that for three different classes of technology a consistent trend in performance is achieved. This must be radically changed to meet goals of future missions such as XEUS. The trend line is perhaps explained by the requirement for increasing mass to support the figuring and alignment of optical surfaces as angular resolution improves.

The key breakthrough needed is to combine a lightweight material which exhibits excellent X-ray reflecting properties, whilst achieving a self-supporting construction that avoids the

distortions inherent in fixation of the optics elements. The progress towards such a breakthrough is reported in this Technical Note, describing a successful proof of concept demonstration of many disparate technology advances across a broad development front.

## 2. Pore Technology – A Hierarchical Assembly

A fundamental feature of the pore optics is that the dimension of an individual pore element, projected over the focal length, defines the angular response. The regular spacing and co-alignment of identical pores can preserve this response and additionally provide a self-supporting assembly. Figure 2 summarises the key geometric parameters of a typical pore optic where the traditional Wolter-1 design is approximated by a conical approximation of two successive sets of pores.

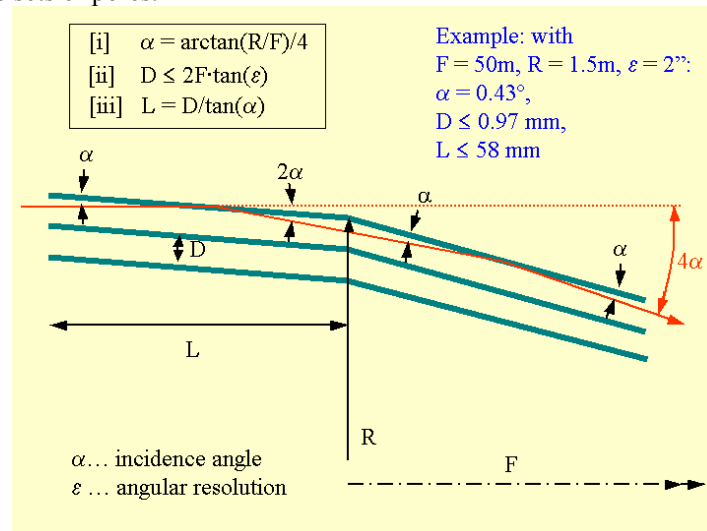


Figure 2. The parameters that define the pore optics implementation of a Wolter-1 conical approximation optics. For a modest focal length and mirror plate radius shown here, arcsecond quality angular resolution requires pore size ( $D$ ) less than 1mm. Conversely a utility factor describing optimised mass of the optics is strongly dependent on focal length via the factors  $L$  and  $\alpha$

We have investigated the use of silicon micromachining techniques developed for the microelectronics industry to enable the formation of such optics prototypes. These technologies enable the fabrication of a complete telescope via a hierarchical assembly process as summarised in Figure 3. Firstly the pores are formed by stacking together a number of silicon plates that have identical rib structures. Two similar stacks are next placed in tandem to approximate a small section of the hyperbola-parabola Wolter pair geometry. Similar stacks are then produced to cover different radii of the telescope and populate a small “petal” element of the complete optical aperture, and the complete telescope built up from a number of identical petals.

The initial stacking process is the most demanding part of the assembly to ensure good optical performance, yet can be achieved with very modest-sized industry standard robotic equipment, which allows a tremendous cost benefit. Thereafter in the hierarchy, the production relies on relatively straightforward mechanical assembly techniques on identically-sized elements. The whole process can therefore be optimised and scaled for the reduction in cost and ready traceability of performance.

By far the most challenging demonstrations have been for the pore production and stacking which we describe next, but the significant achievements towards producing representative final assemblies of the larger hierarchy are also presented.

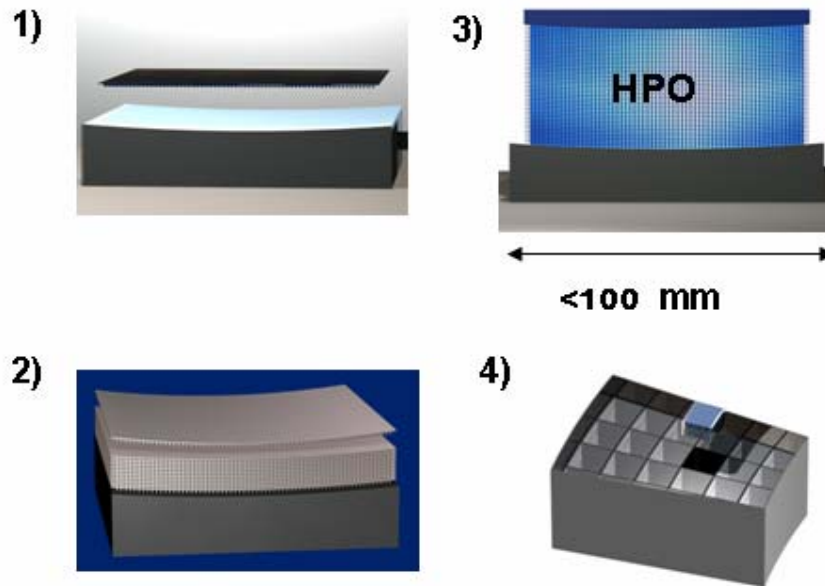


Figure 3 Outline of the hierarchical assembly sequence of pore optics modules. (1) A first Si plate is attached to a precision forming mandrel. (2) Subsequent ribbed plates are stacked to a height of 10's mm. (3) Two sets of stacked plates are placed back to back to form the Wolter-1 tandem pair module (4) The modules are assembled into an optical bench "petal" and aligned within the correct tolerances

### 3. Silicon Ribbed Plates

At an early stage of the activity it was determined that the quality of silicon wafers that are used in the state of art 12 inch lithography has reached an unprecedented level that offers X-ray reflecting quality surfaces as an "off-the-shelf" item (see for example <http://www.siltronic.com/int/noc/Products/Polished/>). There are further advantages to using silicon in producing X-ray optics: silicon is a good thermal conductor and has a low specific mass - a factor  $\sim 4$  lower than electroformed nickel.

Huge investments made in silicon wafer technology and its industrialisation have a long history of development in the electronics industry, including large volume processes for surface chemo-mechanical polishing which can provide the low surface nm scale roughness required for specular X-ray reflection. Commercial requirements of the microelectronics industry have forced wafer manufacturers to fabricate almost atomically flat material with total thickness variations  $<1$  micron over 30cm with extremely smooth surfaces ( $\sim 1\text{\AA}$  rms measured).

Compact chip and sensor (MEMS) technologies have forced the development of attachment techniques in order to build up three-dimensional structures which are used in our technology to achieve a gapless attachment process (processes developed by Qimonda AG). Figure errors of the X-ray optics are therefore ideally reduced to the (small) errors present in the wafer, subject to a particle free environment for assembly.

Relying on this industry investment comes at a price of adopting a standard thickness for silicon plates ( $\sim 800\mu\text{m}$ ). Then subject to the constraints of mechanical strength of the ribs and membrane thickness remaining from the rib excavation, the pore sizes are essentially fixed, with consequent impact on open area ratio and diffraction/geometrical optics resolution limited performance. While some further optimisation of pore dimensions could be attempted, to date attention has focussed on the demonstration of stacking techniques while using a standard pore size that is compatible with arcsecond quality resolution goals.

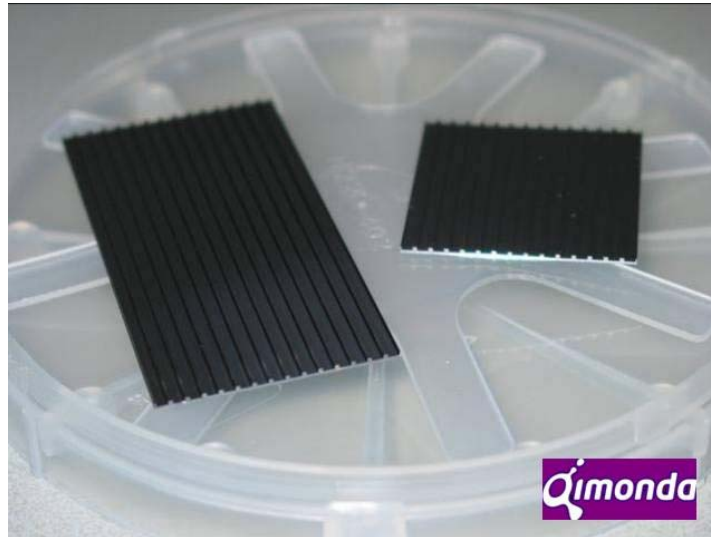


Figure 4 Samples of silicon plates after processing to produce rib structures running vertically and parallel to the wafer edges (courtesy Qimonda AG)

#### 4. Stacking

The demonstration of stacking techniques has been achieved with a compact laboratory robot system installed in a dedicated clean tent environment. Continued development has been necessary to explore and improve disparate issues relating to cleaning and handling of incoming plates, initial bending to a precision mandrel former, metrology for aligning ribs, attachment techniques, metrology for checking plate performance after bonding etc..

An interferometric system is used to check the quality of reflecting surface of each plate following its stacking on the precursor plate, by comparison with a computer generated reference hologram, and with the initial mandrel surface. Figure 6 graphically shows some of the important issues that are being improved upon. Firstly it is seen that cleanliness is absolutely paramount. The assembly conditions must not allow for significant build up of dust particles on the plates, because this causes not only distortions, but locally poor bonding between ribs and plates. This attention to cleanliness must extend also to transport and handling of plates from the supplier.



Figure 5 The laboratory robotic system used for demonstrating the stacking techniques for ribbed Si plates. Image courtesy Cosine Research.

The attachment process requires a highly accurate control of all elements. All the critical movements are controlled with an accuracy of  $\sim 1 \mu\text{m}$  by highly accurate linear stages, a 6-axis degree of freedom tip-tilt stage and a laser alignment system. An imaging system is used to allow the high accuracy determination of the positions, and the image analysis is used to determine and adjust both position and plate bending. During the approach of the plate towards the base, the force distribution is carefully measured so as to control the forces acting and to generate repeatable conditions. Modifications to the mandrel and also to the die used for pressing the plate onto the next stack plate are required to remove the existing problem that prevents the edges of plates properly bonding.

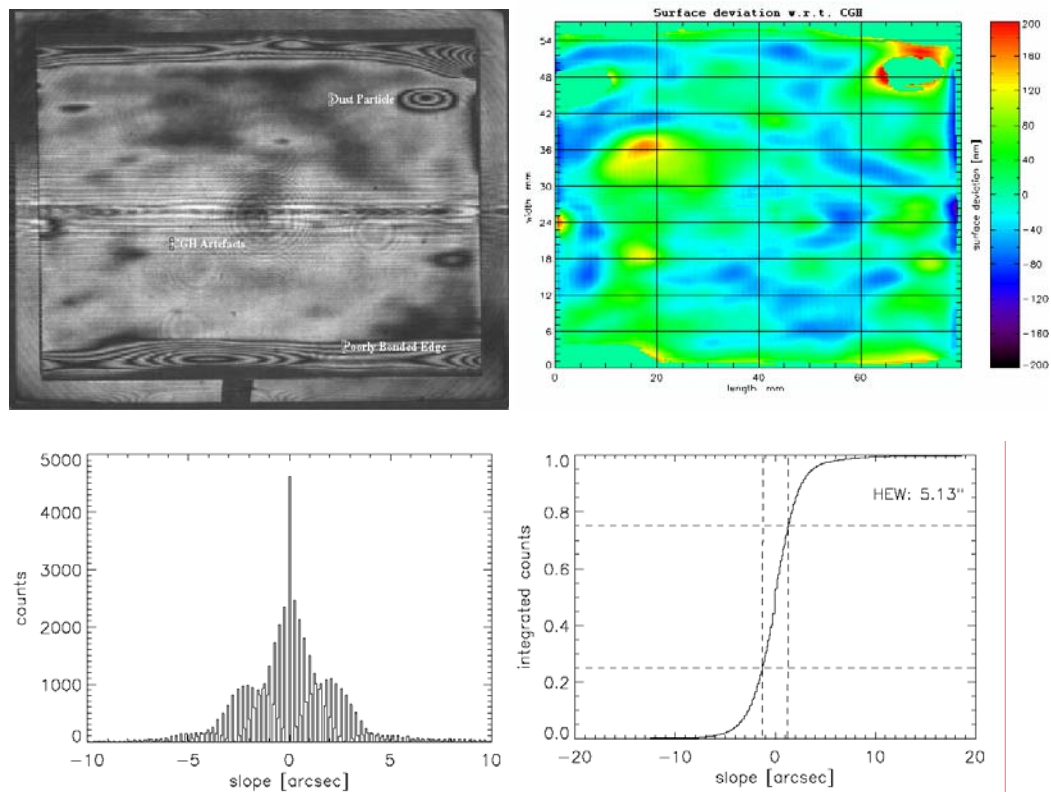


Figure 6 Interferometric measurements collected during the stacking process (courtesy Cosine Research).  
 (a) Top left- the raw interferogram. Features to note include deviations caused by a dust particle on the plate surface to upper right, small artefacts in the computer generated reference hologram (central stripes) which are fixed and always present in the current configuration, and then (along the upper and lower edges of the plate) a region that has not properly been shaped to the initial mandrel due to imperfections in the die plate used in placing the plates on top of each other. Most of the plate is however within a single fringe spacing  
 (b) The resulting deviations from the CGH reference show the majority of the plate lies within  $\pm 40\text{nm}$  of the desired shape, resulting in calculated slope errors (c & d) of much less than 5 arcseconds

Rather than glueing, the simplest method to bond plates relies on a naturally present  $\text{SiO}_2$  layer which forms OH groups on the surface after cleaning. The nature of the bonds can be further modified a heat treatment. Extensive investigations have been carried out into the relative merits of hydrophillic and hydrophobic bonding and several techniques explored to increase the bond strength.



*Figure 7 Assembled stack located in measurement jigs prior to scanning tests at the PTB laboratory int BESSY. This particular stack comprises 35 plates*

## 5. Wedging

Until recently most of the efforts were concentrated on this production of simple plane parallel stacks. However from Figure 2 it can be appreciated that for proper focussing, the angle  $\alpha$  must be accommodated between plates. This is achieved by structuring the ribs with a slight height change from end-to-end of the plate (~micron over 70mm plate length). Various combinations of etching and oxidation processes have been investigated, and now it is possible to achieve a reliable plate-to-rib bond after wedging to the required angle.

## 6. Tandem Production

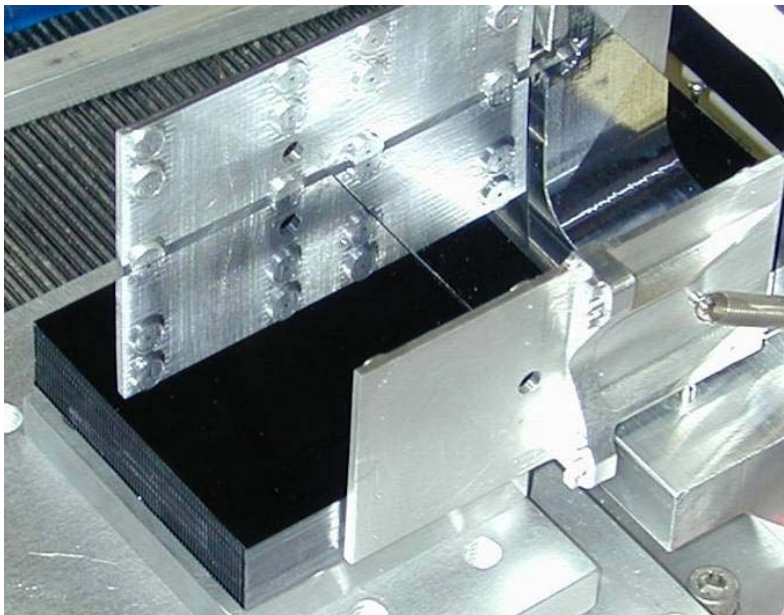


*Figure 8 Close-up view of first XOU tandem being integrated into a test aluminium bracket (eventually all brackets will be in CeSiC for best thermal match and mass reduction requirements). This picture allows visibility of the guide structures used to ensure precision glueing, which are not visible in the following Figure 9*

As part of the overall HPO production chain we have now been investigating the assembly of stacks into tandems (a.k.a. XOUs) and tandems into optical bench petals. The objective has been to establish a low mass accommodation design and to demonstrate reliable fixation and

alignment techniques. The concept relies on careful alignment of two stacks within a bracket and precision glueing. Figure 8 shows a partially assembled tandem. In this case a small incomplete stack was used in a demonstration aluminium bracket in order to test out the alignment concept. A dedicated X-ray beam line at the PTB laboratory in BESSY is used to aid the alignment between the stacks which is required to be better than  $\sim 100\mu\text{m}$  in translation and  $<20^\circ$  in rotation.



Figure 9 Second completed XOU tandem, now integrated into a low mass CeSiC bracket representative for flight-like design

## 7. Petal Prototype

A prototype optical bench petal has been designed and fabricated. The aim of this activity being to demonstrate techniques for integration of XOUs into a flight representative optical bench, as well as to explore the feasibility of thermal design and mass optimisation. Figure 10 shows a close up of sections of the prototype petal after initial sintering of the CeSiC green body



Figure 10 Sintered CeSiC prototype optical petal demonstration unit. Images courtesy of Kayser Threde

Interface points for mounting the XOU modules are subsequently polished into the CeSiC structure, and metrology of the structure conducted to confirm the geometry of the petal is adequately met. (Figure 11)

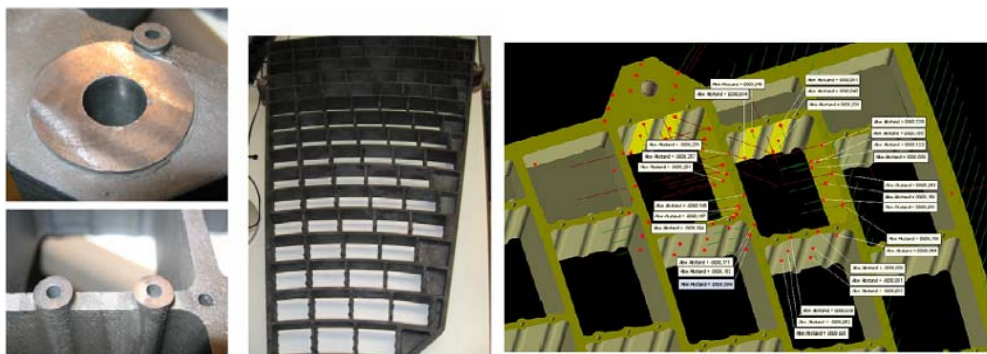


Figure 11 Left – close-up of interface points on the petal structure after polishing. Right- location of metrology points measured in preparation for mounting the first of the XOu tandem units Images courtesy Kayser Threde

## 8. Coatings

The naked silicon surface does not offer acceptable reflectivity, particularly at high energies  $>2\text{keV}$ . To meet the science requirements for effective area at 6-7keV will need a high atomic number surface coating. The ability to coat Si with a coating such as gold has now been demonstrated. The Si surface must be prepared to prevent gold migration, and a thin Ti layer was used to improve adhesion. The reflectivity versus graze angle at 8keV was measured and in Figure 12 is compared with the predicted values

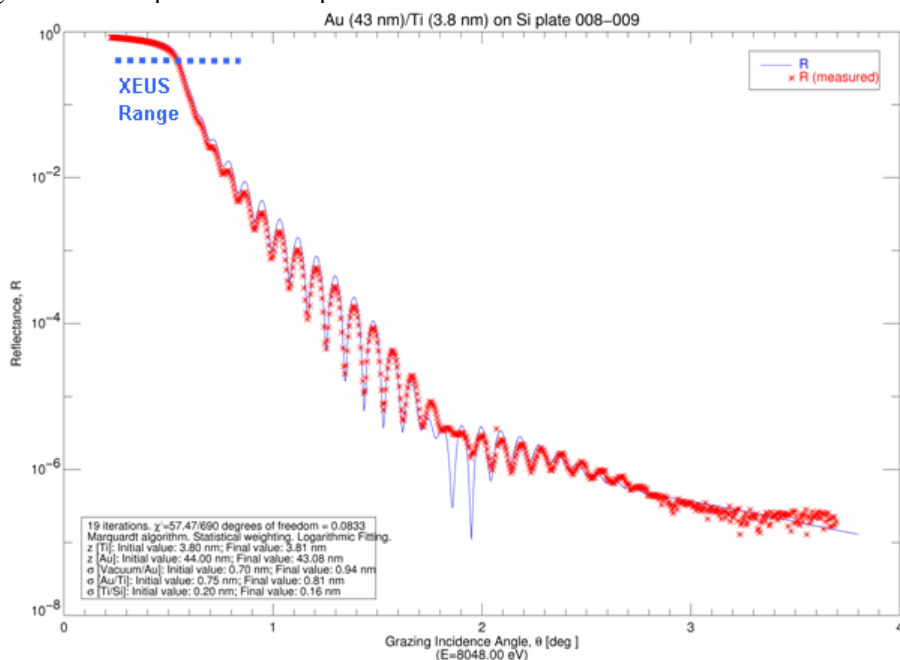


Figure 12 Measured (red) reflectivity of Au coated Si plate versus graze angle at an energy 8keV. The light blue line is the best fit theoretical prediction accounting for layer thicknesses and roughness. Deposition and data courtesy SRON

An additional complication is that such coatings cannot easily be introduced onto the reflecting surface once the stack is introduced. Coating the plate before stacking also precludes the natural bonding process, so that the areas for rib bonding must be masked from the coating. Figure 13 shows a successfully coated plate that has had a lithographically masked area defined from which the coating was not applied. It remains to be established that such plates can be successfully bonded, especially without introduction of further particulate contamination from the lithography process that may impede bonding.

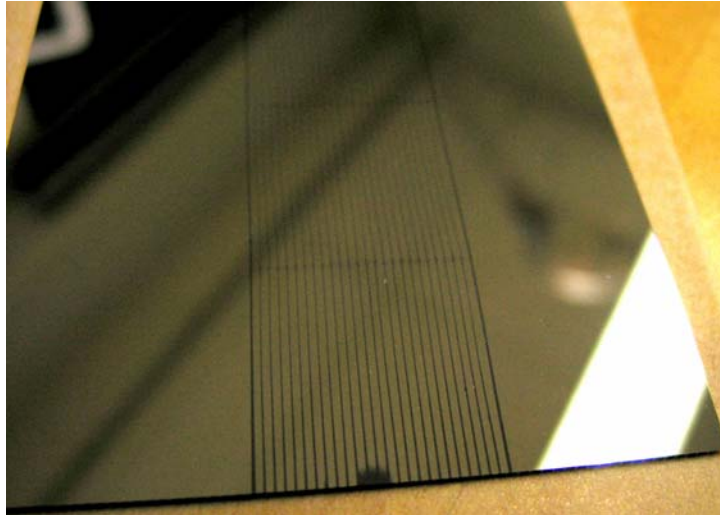


Figure 13 Sample Si plate that has been lithographically masked and then coated with a Tungsten reflecting coat. Areas for rib adhesion are clearly visible, running vertically. Depositions and image courtesy of Danish National Space Center.

The reflectivity of gold is well-understood from many previous X-ray telescope applications. However some activities have been carried out to try and optimise the effective collecting areas to higher performance than achievable with gold. Above 10keV, depth-graded multi-layers offer the capability of much enhanced reflectivity. A development activity with industry has been completed with the aim of demonstrating coating capability and subsequent reflection performance on representative silicon plates. A study on depth-graded coatings optimised for 20-70keV (albeit based on old XEUS-1 configuration) was completed. W/Si and Mo/Si of typical designs were deposited on representative Si substrates. Typical coatings comprised ~300 bi-layers ranging from 3-30nm in thickness. The typical deposited layer roughness was found to be ~0.5nm. Trials were also conducted to extend the technology with up to 600 bi-layers as thin as 2.5nm, In addition we investigated buffer layers and deposition gas compositions to compare routes for maintaining good roughness scales.

Figure 14 shows the measured reflectivity of two multi-layer designs and compares their performance with a theoretical prediction for gold.

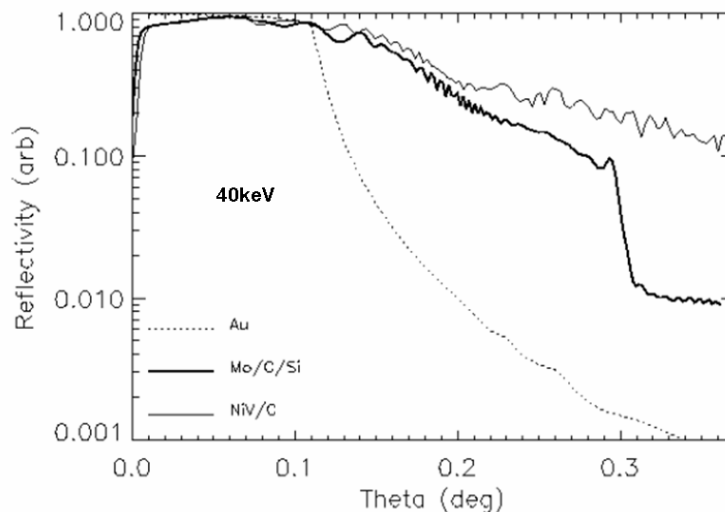


Figure 14 Measured reflectivity of two multi-layer designs at an energy of 40keV. A substantial increase compared with gold is achievable. With the current XEUS design, the inner radius corresponds with a grazing angle of ~0.25 degrees, therefore factors of several reflectivity improvements can be achieved with careful multi-layer design. Depositions and data provided courtesy XENOCs, Danish National Space Center and PTB / BESSY

Pareschi et al proposed using a C over-coat on conventional metal layers to increase reflectivity at low energies. As we already were investigating Pt/C multi-layers, an extension of the study was made to deposit 10nm C on top of a 100nm thick Pt reflector. The measured reflectivity vs energy at a typical graze angle  $\theta = 10$  mrad and for reflectivity vs  $\theta$  at single energy were obtained. Figure 15 highlights the significant improvement attainable in the range 1 – 5 keV.

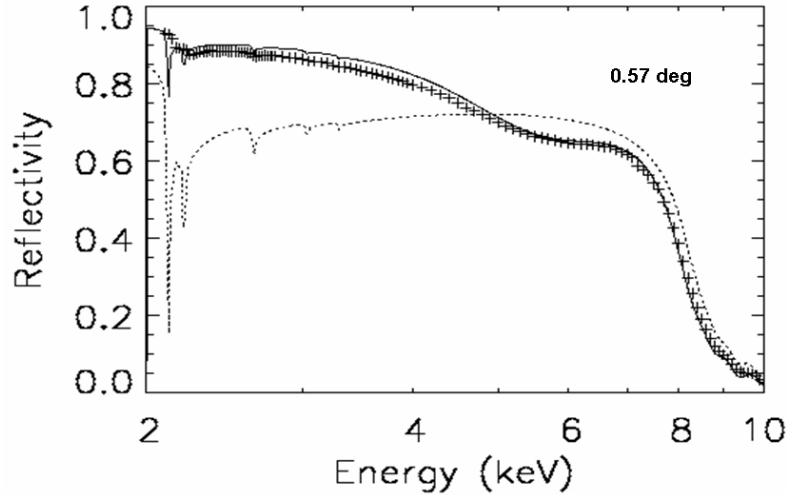


Figure 15 Measured reflectivity of a carbon-overcoated Pt reflector measured at a typical XEUS graze angle, and a range of energies. (Theory bare Pt ..... Theory C-Pt \_\_\_\_\_ Measured C-Pt + + + + ). Depositions and data provided courtesy Danish National Space Center and PTB / BESSY following an idea by G Pareschi et al

A combination of multi-layer coatings on the inner mirrors and carbon coated iridium on the outer mirror radii seems to offer the best compromise to meeting the XEUS science requirements of effective area at different energies. Figure 16 shows a typical effective area that might be achieved for a geometric design for  $0.67 \text{ m} < R_{\text{mirror}} < 2.1 \text{ m}$  and with effective dead area fraction that is achievable based on existing petal blocking fractions and possible pore open area ratios.

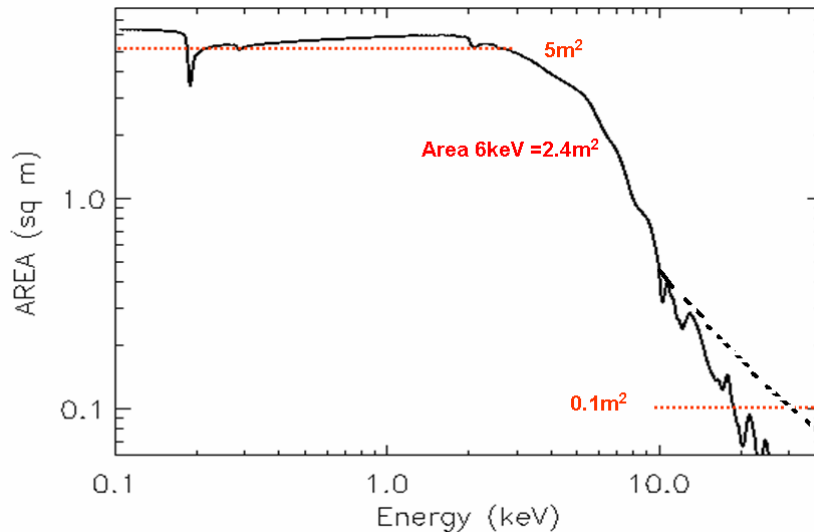


Figure 16 Predicted effective area vs. energy for a XEUS mirror design based on  $0.67 < R < 2.1$  metres, and feasible dimensions of pore optics filling factor. A carbon coated Ir reflecting surface was adopted, except for an inner section with a multilayer coating. Science requirements for area at 1 and at 10keV are indicated (5 and  $0.1 \text{ m}^2$ ). The dotted black line indicates that improvements in multi-layer design with very thin bi-layers could potentially reap further benefits.

## 9. Pencil Beam Measurements

Verifying the performance of prototype optics has been difficult to execute with a traditional full-beam illumination for a number of reasons, including the fact that most modules have not been fabricated in a focussing Wolter-1 configuration, the focal length is prohibitive for true focussing measurement in any facility available, especially considering the diverging beam constraints, and finally the complications of interfacing, availability and feedback time for results. Therefore we have arranged for dedicated measurements on a beam line at the PTB laboratory in the BESSY synchrotron facility which has the advantages of

- Almost permanent availability
- High flux and negligible beam divergence and spot size complications
- Dedicated 6 d-o-f manipulator also allows alignment and fixation to be attempted on-site with near-real time X-ray data verification

The pencil beam testing is carried out at an energy of 2.8 keV, with a spot size that is varied in the range 0.05 – 2 mm. The reflected beam is measured at a distance of 5m by a 1300 x 1300 pixel CCD system with  $\sim 1''$  resolution. Autocollimators are used as an external reference to control and readout the automated 6-axis scanning system with high spatial resolution. Not only does this system allow the probing of an optics module for localized fault examination, it allows via beam superposition to simulate a full-beam result without deconvolution. Figure 17 shows the beam line chamber opened to reveal the scanning tables, and an explanation of a typical beam scan.

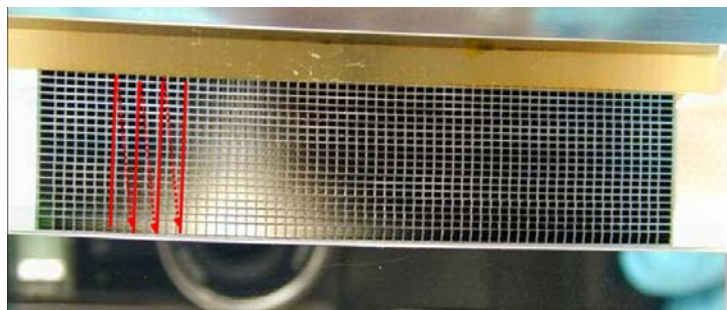


*Figure 17 (Upper) Small optics module stack located on top of 6-axis precision table inside beamline chamber at the PTB Laboratory in BESSY. (Lower) the red solid line traces the path of the pencil beam that can track along each pore. For example a 50micron spot projected over a typical graze angle can intercept the whole pore by illuminating  $\sim 10$  successive steps, and then laterally a comparable number of locations per pore. The same pattern can be repeated for every single pore of the stack, or used to probe peculiarities of individual pores.*

One of the most important uses of the scanning technique is to investigate the properties of the plate stacking and verify that the overall X-ray response is comparable with the predictions derived from the interferometric metrology accumulated during assembly. The known errors of the first plate of a stack, that are due to edge defects as a result of poor die pressure distribution and some remnant mandrel deficiencies, can be verified by scanning the

first plate with the pencil beam. Subsequent plate pencil beam scans can be compared with this first reference scan, and any additional accumulation of stacking errors directly assessed. Figure 18 shows a typical result of such analysis.

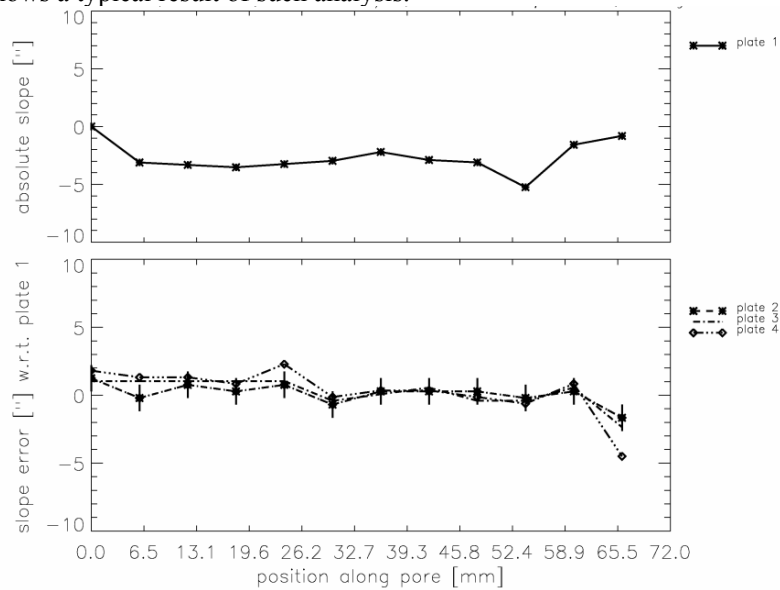


Figure 18 (upper) shows the absolute slope errors along the pores of one plate, taken at some distance from known mandrel edge defects. (Lower) comparable scans for the next 3 plates are shown, after removal of the absolute slope errors of the reference plate. This gives an indication of the **build up** of additional slope error during stacking. All data courtesy Cosine Research and PTB / BESSY

More graphically the data may be recast (Figure 19) by superimposing the data comprising ~1000 beams each. The image spots are not re-centred but displaced only accounting for input beam shifts. Longitudinal slope errors account for most of the distortion into one direction. Nevertheless the 50% encircled energy width is equivalent to 8 arcseconds on the first plate, degraded only to 8.8 arcseconds in 3 plates. No reduction for finite beam sizes has been made.

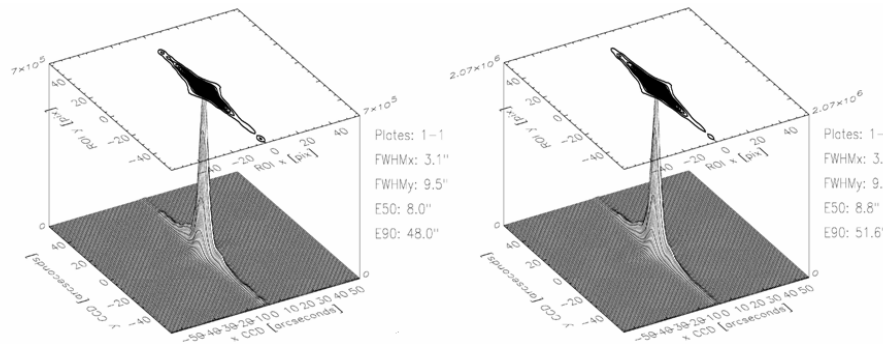


Figure 19 The data such as Figure 18 may be recast as 2-dimensional PSFs. 90% of the whole available area of the plates are sampled (leaving out only the defective unbonded plate edge areas) No account is taken of the initial mandrel figure errors

To appreciate the attainable performance that might be realised after accounting for a perfect mandrel, Figure 20 shows the equivalent data for 6 successive plates after the reference data of the first plate (affected by poor mandrel performance or edge bonding) have been removed.

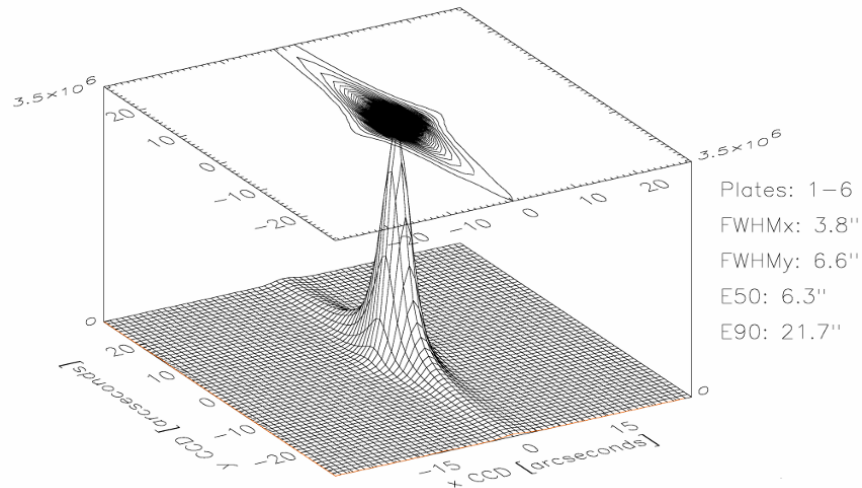


Figure 20 Superposed image spots after removing first plate reference distortion. After quadrature subtraction of the finite beam size, the Half Energy Width is determined to be ~5.5 arcseconds

Finally we plot the equivalent data newly obtained for the first pencil beam measurement of a tandem stack after two reflections. The HEW is in this case 3.8 arcseconds or 2.2 arcseconds after quadrature subtraction of finite input beam

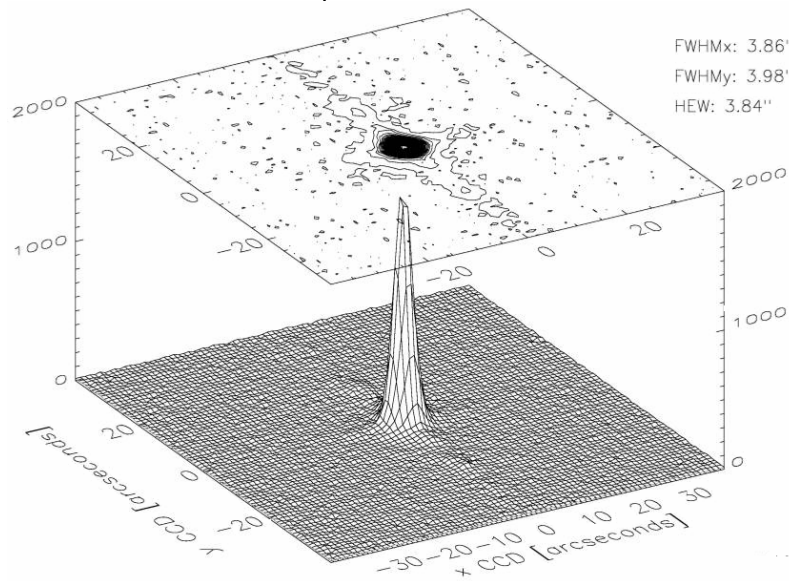


Figure 21 Pencil beam illumination of the first Tandem module fabricated for the demonstration petal. HEW after beam subtraction is 2.2 arcsecs HEW. Mandrel reference scan removed.

## 10. Full Beam Measurements

Per interim the unavailability of focussing modules has reduced the utility of carrying out full beam tests. However preparations are underway to establish a beam condenser for arcsecond quality parallel beams for future tests at the Max Planck Panter facility. Therefore as part of the preparation, a number of pore optics modules have been tested at Panter. While these are primarily to test procedures and interfaces, the initial data look promising and are to be further analysed to check for verification of the superposition analysis of the pencil beam measurements'



Figure 22 HPO stack module placed inside Max Planck Panter chamber for the purpose of checking interfaces for future full beam illumination tests. Image courtesy MPE.

Figure 22 shows an image acquired at the Panter during these interface tests, highlighting some artefacts of the data.

## 11. Summary and Future Activities

Significant advances have been made on all aspects of demonstrating the key fabrication challenges of the High Precision Pore Optics concept. These include:

- Silicon wafers developed for 12" industry standard foundries have the surface polish and figure accuracy necessary to meet XEUS requirements
- Silicon plates can be coated with conventional reflecting materials (e.g. Au) with a lithographic masking to allow coating before the stacking process
- Coatings have been developed to allow a measure an optimisation at low energies (C overcoat) and for the highest energy ranges (>10keV via. depth graded multilayers)
- Silicon plates can be machined to provide pore sizes commensurate with geometrical and diffraction limits that allow the 2 arcsec goal resolution to be reached
- Silicon ribbing can be accomplished with an added wedge shape to allow the appropriate geometry for focussing
- Stacking of Si ribbed plates onto a mandrel can demonstrate reproduction of the required shape up to stack heights of 10's of plates, limited only by initial mandrel quality and ability to press the plates with uniform pressure
- Annealing techniques have been explored to establish the optimum parameters for guaranteeing good bond strength
- HPO plate stacks can be aligned with required accuracy into a tandem XOu module with the appropriate Wolter – 1 approximating geometry
- XOu tandems can be installed into a representative light weight optical bench petal with a minimal mass and dead area loss
- Measurement techniques have been developed to demonstrate and verify performance at all stages of the fabrication and integration processes, using combinations of optical metrology, X-ray pencil beam and full beam illumination testing

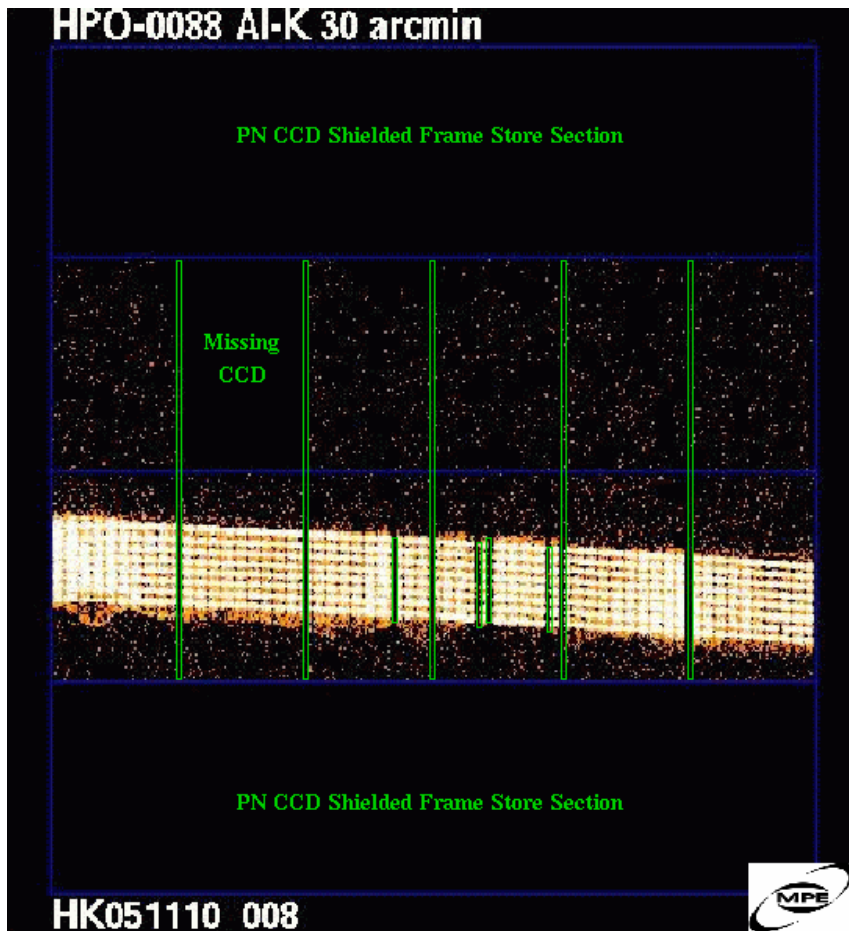


Figure 23 Data taken using the Panter with the Flight Spare XMM EPIC PN Camera. Logarithmic scaling Blue rectangles delineate the CCD peripheries. Green rectangles highlight the inter-CCD gaps and dead CCD columns. The upper CCD half has image data containing background events experienced within the chamber. The HPO module was illuminated at an angle of 30 arcseconds and shadows of the stack structure can be seen as narrow vertical dark lines caused by the ribs of the plates, with equivalent pseudo-horizontal lines caused by the plates themselves. To the left one can see anomalous reflections from distorted portions of plates (albeit at low surface brightness). Some variation in throughput along the stack may result from reflectivity changes, dust obscuration or other contaminant blocking.

Notwithstanding all these successes, further modification, refinement and developments have been identified for all phases of fabrication and integration in a sustained manner that must be achieved if the overall requirements of XEUS in respect of angular resolution and effective area can be met within engineering constraints identified in system level accommodation studies.

#### Acknowledgements

This wide ranging set of activities was carried out in cooperation between ESA and a large number of industry and research group partners. We especially acknowledge the contributions of Cosine Research, Kayser Threde, Qimonda, Wacker Siltronics, SRON, PTB, BESSY, Danish National Space Center, XENOCSS and Max Planck Inst. Fur Extraterrestrischephysik.